Dynamic Monte Carlo Simulation of Olefin Polymerization in Stopped-Flow Reactors

João B. P. Soares, Tuan Nguyen*

Summary: Stopped-flow reactors are very useful to estimate olefin polymerization rate constants and to investigate particle morphology development. Because the residence time in these reactors is comparable to the life time of the polymer chains, very narrow molecular weight distributions are obtained and the number average molecular weight is proportional to reactor residence time. In this case, traditional models for olefin polymerization in industrial reactors can not be applied. In this contribution, we derived analytical solutions and performed Monte Carlo simulations to describe the time evolution of the molecular weight distribution of polyolefins made with single- and multiple-site catalysts in stopped-flow reactors.

Keywords: monte carlo simulation; polymer reaction engineering; polyolefins; polypropylene; stopped-flow reactors

Introduction

Polyolefins are produced in several types of industrial processes. Most processes use reactors that have residence times of one or more hours, which are a few orders of magnitude higher than the lifetime of a polyolefin molecule. Solution olefin polymerization processes generally have shorter residence times of five to ten minutes, but they are still significantly higher than the lifetime of polyolefin chains. Under these conditions, the steady-state hypothesis (SSH) is valid and the molecular weight distribution (MWD) can be described with one (for single-site catalysts) or several (for multiple-site catalysts) Flory's most probable distributions.[1,2] In stopped-flow reactors, however, the residence time varies only from tenths of seconds to a few seconds. Under these conditions, the SSH is violated and the MWD is not described by Flory's distribution.[3]

A stopped-flow reactor was first used for olefin polymerization by Terano et al. in 1987[4] and has since then been applied to help elucidate several aspects of olefin polymerization kinetics and particle morphology development with coordination catalysts during the first seconds of polymerization.[5–8] This technique is important for the fundamental understanding on how coordination catalysts work, but there is a lack of quantitative predictions on how polymer chains grow during these first seconds of polymerization. In this paper we present three models to describe polymerizations with coordination catalysts under such short residence times: in Model 1 we assume that the reaction between catalyst precursor and cocatalyst molecules to form active sites is instantaneous; in Model 2 we relax this previous assumption; finally, in Model 3, we assume a continuous distribution of active site types over the surface of the catalyst.

Figure 1 shows a diagram of a stopped-flow reactor. In a typical configuration, catalyst and co-catalyst are pre-contacted with monomer and the diluent in separate vessels and mixed before being introduced in the tubular reactor. By varying the flow rate of reactants, the residence time in the reactor is easily changed.

Table 1 lists the polymerization mechanism adopted in this work. We kept the

Department of Chemical Engineering, University of Waterloo, Waterloo, Ontario, Canada N2L 3G1
E-mail: jsoares@uwaterloo.ca

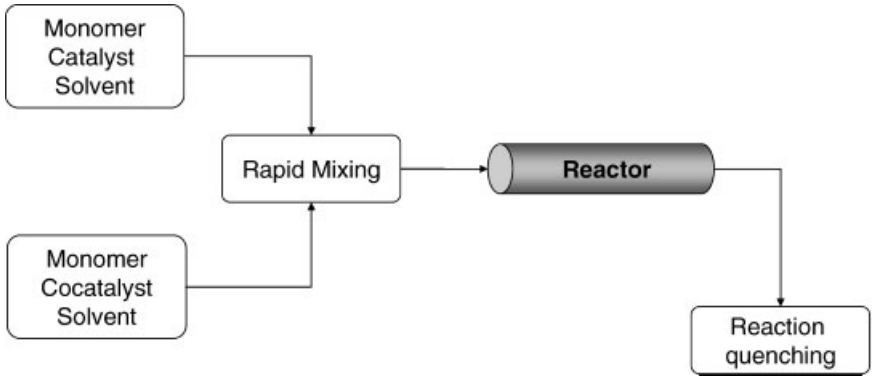

Figure 1.
Schematic of a stopped-flow reactor.

model as simple as possible by adopting a single chain transfer step (to a small molecule *X*), but the model could be easily extended to include more transfer steps without changing our conclusions. This model can also be used for copolymerization, by replacing the kinetic constants with copolymerization pseudo-kinetic constants[2] without losing the generality of our conclusions. In the following sections we will show only the final model equations based on this polymerization mechanism; model derivation details have been published elsewhere.[3,9]

Model 1: Instantaneous Active Site Formation

In Model 1, we assume instantaneous reaction between catalyst precursor (*C*) and cocatalyst (*Al*) molecules to generate active sites (C^*). Solving the population balances for living and dead polymer chains, we obtain the following set of model equations:[3]

$$f_r^L = \frac{p_p^{r-1}}{1-\exp(-\alpha t)}\left\{p_t\left[1-\frac{\Gamma(r,\alpha t)}{\Gamma(r)}\right]+p_p\frac{(\alpha t)^r}{r!}\exp(-\alpha t)\right\} \quad (1)$$

$$f_r^D = \frac{p_p^{r-1}}{\alpha t+\exp(-\alpha t)-1}\left\{p_t\left[\alpha t - r + \frac{\Gamma(r-1,\alpha t)(1-r)(\alpha t - r)+\exp(-\alpha t)(\alpha t)^{r-1}r}{\Gamma(r)}\right] + p_p\left[1-\frac{\Gamma(r,\alpha t)}{\Gamma(r)}\right]\right\} \quad (2)$$

where f_r^L and f_r^D are the number chain length distributions for living and dead chains, respectively. The probabilities of propagation and termination, p_p and p_t, are defined as:

$$p_p = \frac{k_p[M]}{\alpha} = \frac{k_p[M]}{k_p[M]+K_t} \quad (3)$$

$$p_t = \frac{K_t}{\alpha} = \frac{k_t[X]}{\alpha} = \frac{K_t}{k_p[M]+K_t} \quad (4)$$

Table 1.
Polymerization mechanism.

Elementary Step	Chemical Equations
Activation	$C + Al \xrightarrow{k_a} C^*$
Initiation	$C^* + M \xrightarrow{k_p} P_1$
Propagation	$P_r + M \xrightarrow{k_p} P_{r+1}$
Transfer	$P_r + X \xrightarrow{k_t} C^* + D_r$

C: catalyst precursor, C^*: active site, *Al*: cocatalyst, *M*: monomer, P_r: living chain of length *r*, D_r: dead chain of length r, *X*: chain transfer agent.

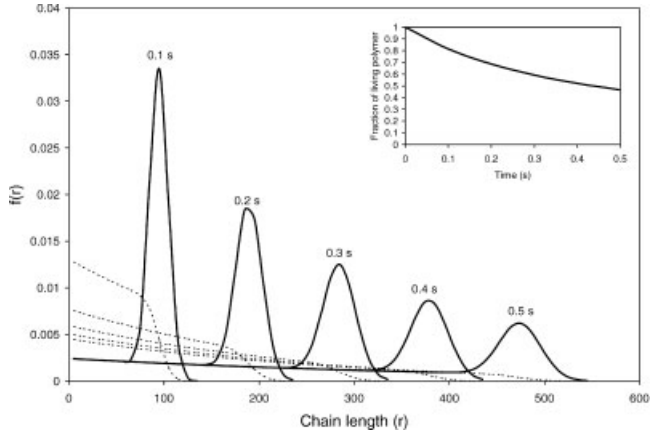

Figure 2.
CLD for living (solid lines) and dead (dotted lines) polymer chains as a function of residence time in a stopped-flow reactor. Model parameters: $p_p = 0.9976$, $p_t = 1 - p_p$, $\alpha = 952.3\ s^{-1}$.

Finally, the gamma and gamma complementary functions are defined as:

$$\Gamma(r) = \int_0^\infty e^{-x} x^{r-1} \mathrm{d}x \tag{5}$$

$$\Gamma(r, \alpha t) = \int_{\alpha t}^\infty e^{-x} x^{r-1} \mathrm{d}x \tag{6}$$

Figure 2 shows how the chain length distribution (CLD) of a model polymer varies as a function of residence time in a stopped-flow reactor. In is interesting to see that the CLD for the dead polymer always lags behind the CLD for the living polymer, which moves as a polymerization front through time. This is just a consequence of the short polymerization times, which means that the dead polymer has not had time to reach its fully developed CLD. Notice also how the fraction of living chains decreases as a function of polymerization time. If we wait long enough, the CLD of

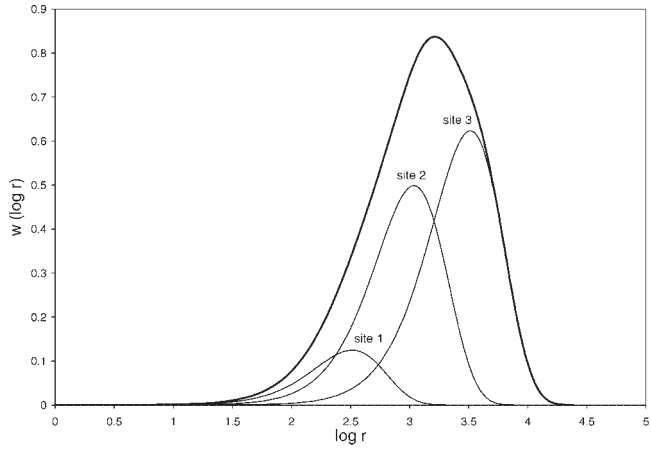

Figure 3.
CLD of a polyolefin made with a 3 site-type catalyst. Model parameters: $x_1 = 0.37$, $x_2 = 0.44$, $x_3 = 0.19$, $k_{p1}M = 375\ s^{-1}$, $k_{p2}M = 1250\ s^{-1}$, $k_{p3}M = 3750\ s^{-1}$, $K_{t1} = K_{t2} = K_{t3} = 2.299\ s^{-1}$ (x_i is the mass fraction of chains made by site type i).

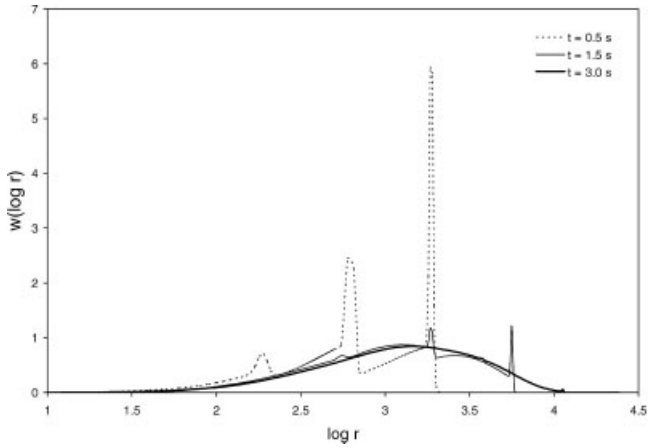

Figure 4.
CLD time evolution for polymer made on a three site-type catalyst. Simulation parameters are given in Figure 3.

both living and dead polymer will eventually become Flory's most probable distribution.[3]

This treatment can be extended to multiple-site catalyst if we assume that the CLD of polymer made with them can be represented as a superposition of several distinct Flory's CLDs.[2] Figure 3 shows the steady-state CLD of a model polymer made with a three site-type catalyst; the steady-state CLD conforms to what we normally measure experimentally, but its time evolution, as it passes through a stopped-flow reactor, is clearly not realistic, as illustrated in Figure 4. A possible reason for this disagreement with experimental results is the assumption of instantaneous site activation made in Model 1. We will see below that when this hypothesis is relaxed in Model 2, the predicted CLDs approximate much better experimental results.

Model 2: Non-Instantaneous Active Site Formation

For the case on non-instantaneous site activation, the following equations are obtained for the dynamic CLDs of living and dead polymers:[9]

$$f_r^L = p_p^r \frac{\frac{\kappa_a - p_t}{(1-\kappa_a)^{r+1}}\exp(-\alpha\kappa_a t)\left[1 - \frac{\Gamma[r+1,\alpha(1-\kappa_a)t]}{\Gamma(r+1)}\right] + p_t\left[1 - \frac{\Gamma(r+1,\alpha t)}{\Gamma(r+1)}\right]}{1 - \exp(-\alpha\kappa_a t) - \frac{\kappa_a - p_t}{1-\kappa_a}[\exp(-\alpha\kappa_a t) - \exp(-\alpha t)] - p_t[1 - \exp(-\alpha t)]} \tag{7}$$

$$f_r^D = p_p^{r-1} \frac{\left\{\begin{array}{c}\frac{\kappa_a - p_t}{\kappa_a(1-\kappa_a)^{r+1}}\left[(1-\kappa_a)^{r+1} - \exp(-\alpha\kappa_a t) + \frac{[\exp(-\alpha\kappa_a t)\Gamma[r+1,\alpha t(1-\kappa_a)] - (1-\kappa_a)^{r+1}\Gamma(r+1,\alpha t)]}{\Gamma(r+1)}\right] \\ + p_t\left\{\alpha t - \left[r + 1 - \frac{\Gamma(r+1,\alpha t) - \alpha t\Gamma(r,\alpha t)}{\Gamma(r)}\right]\right\}\end{array}\right\}}{\alpha t - \frac{1-\exp(-\alpha\kappa_a t)}{\kappa_a(1-\kappa_a)} + \frac{\kappa_a[1-\exp(-\alpha t)]}{1-\kappa_a}} \tag{8}$$

where $\kappa_a = k_a[Al]$. These equations are extensions of Equation (1) and (2) for the case of non-instantaneous activation.

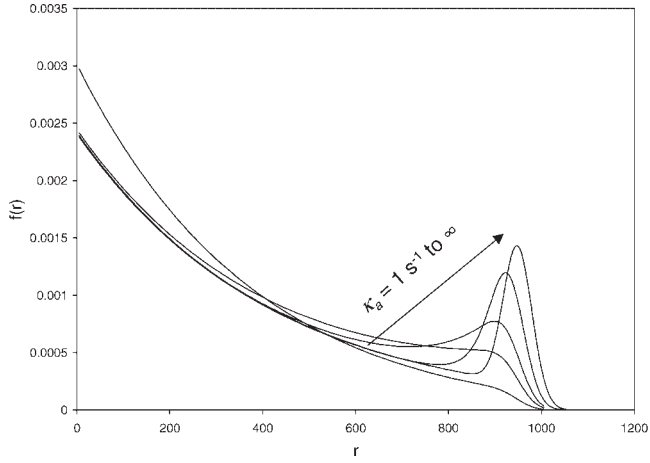

Figure 5.
Effect of site activation rate on the dynamic evolution of the CLD of live and dead chains after five seconds of polymerization. Model parameters: $k_pM = 950\ s^{-1}$, $k_tX = 2.3\ s^{-1}$, $p_p = 0.9976$.

Figure 5 shows that, as κ_a decreases (that is, site activation slows down), the CLD flattens out, since the catalytic sites do not all activate at the same time and the polymer chains do not start growing simultaneously.

Interestingly, even for the case of non-instantaneous site activation, we still observe a linear relationship between number average chain length (or number average molecular weight) and time for short polymerization times before the SSH becomes established. This is clearly demonstrated in Figure 6 and proves that the experimental observation of this linear relationship is not guarantee of instantaneous site activation.

Interestingly, Figure 7 shows that when the activation of catalyst sites is not instantaneous in a multiple-site catalyst, the CLD evolves in time without the appearance of the sharp peaks shown in Figure 4 for instantaneous activation. Since experimentally measured CLD of polymers made in stopped-flow reactors do not show the sharp peaks predicted in Figure 4,

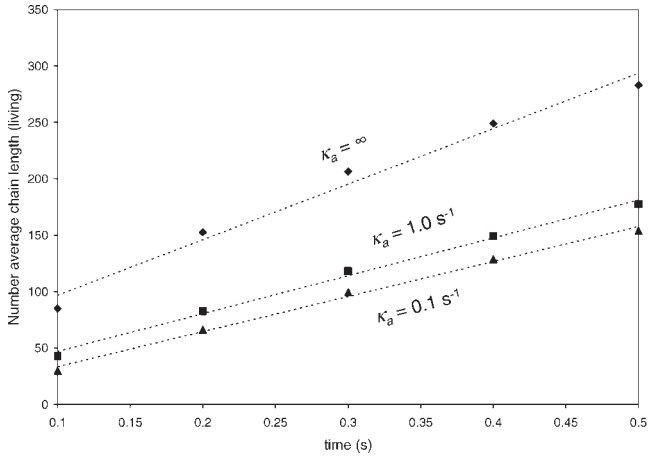

Figure 6.
Influence of site activation rate the time evolution of the number average chain length of polymers made in stopped-flow reactors.

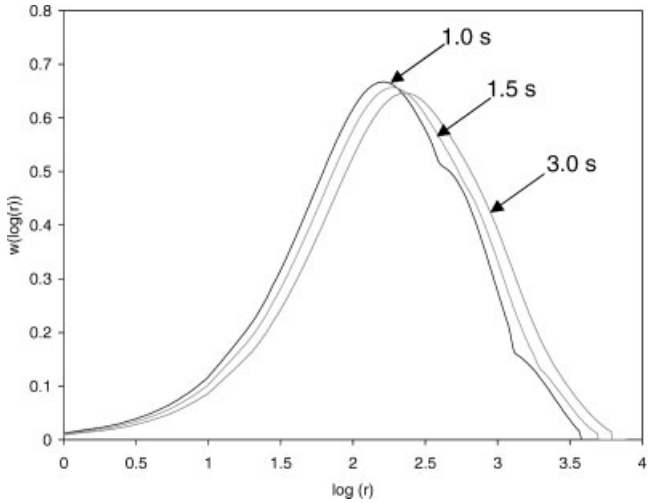

Figure 7.
CLD time evolution for non-instantaneous activation. Simulation parameters are the same as in Figure 3, with $\kappa_{a1} = \kappa_{a2} = \kappa_{a3} = 0.1\ s^{-1}$.

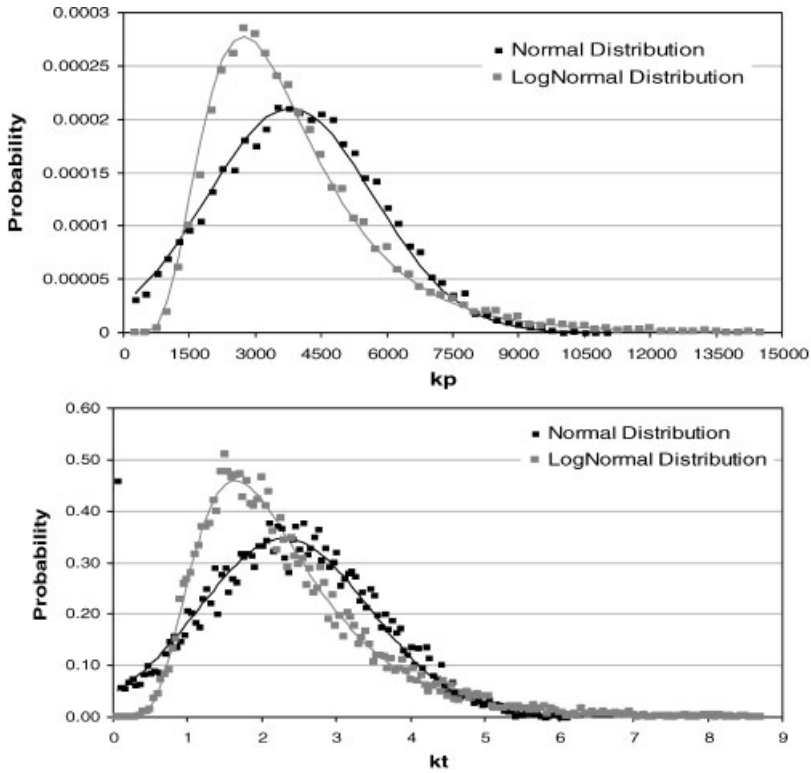

Figure 8.
Normal and log-normal distributions for k_p and k_t. The mean value and standard deviation for k_p are $k_{p,\mu} = 3800$ L/mol.s and $k_{p,\sigma} = 1900$ L/mol.s. Similarly, for chain transfer, $k_{t,\mu} = 2.3\ s^{-1}$ and $k_{t,\sigma} = 1.15\ s^{-1}$. The solid lines are the analytical distributions and the square dots are Monte-Carlo generated samples of the respective distributions.

this seems to lend support to the non-instantaneous site activation hypothesis adopted in Model 2.

A note of caution is required at this point: most multiple-site catalysts are heterogeneous. In this case, the time constant required for cocatalyst to diffuse to the catalyst sites is comparable to the residence time in a stopped-flow reactor. In this case, the site activation may not be instantaneous for simply physical, not chemical, reasons. That is, the site activation reaction itself may be very fast, but the time required for the cocatalyst molecules to reach the catalyst sites within the catalyst support will slow down site activation and lead to similar predictions of a slow active site activation rate.

Model 3: Continuous Distribution of Active Sites

Our last model is more speculative than the previous two and applies only to multiple-site catalysts. In Model 3, we assume that multiple-site catalysts are not modeled as a superposition of single site catalysts, as proposed in Figure 3, but result from a continuous distribution of polymerization kinetic parameters from site to site. Such distribution could arise, for instance, from a distribution of crystal imperfections on supported catalysts, steric and electronic effects due to the proximity of other active sites, and different modes of coordination with cocatalysts and donors. Mathematically, this means that the values of the three kinetic constants used in the mechanism shown in Table 1, k_a, k_p, and k_t, will not have a single value, but will follow a given statistical distribution such as normal or log-normal, for instance. A similar idea was proposed by Soares in a previous publication.[10]

For simplicity, we will assume that active site formation is instantaneous in Model 3, since we want to focus our attention on the effect of distributed values for k_p and k_t only. In this case, an analytical solution can

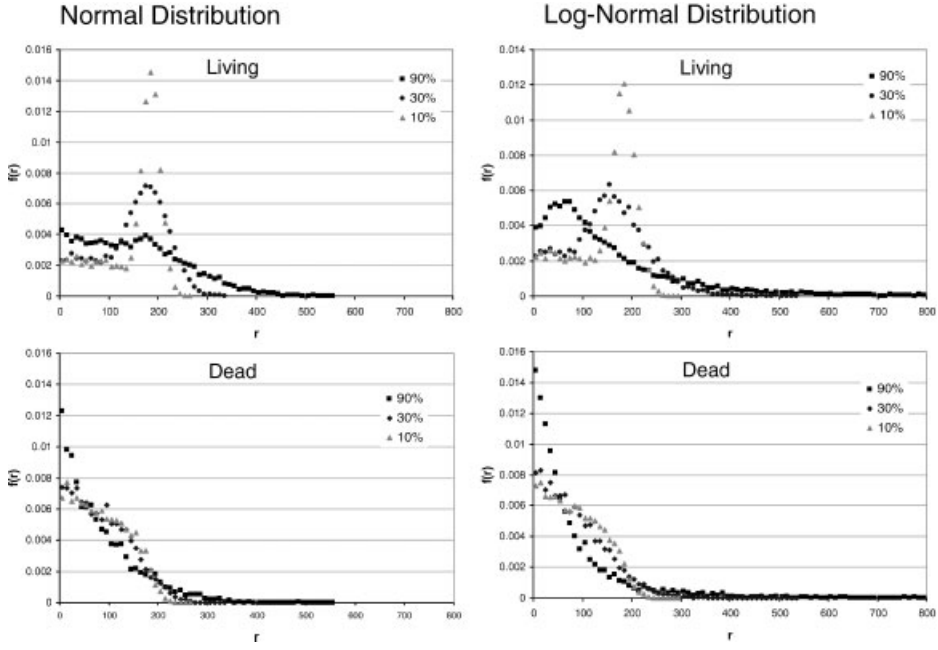

Figure 9.
Effect of increasing the standard deviation of k_p and k_t on the CLD of polymers made with a single site catalyst in a stopped-flow reactor with residence time of 0.2 s. Model parameters: $k_{p,\mu} = 3800$ L/mol.s and $k_{t,\mu} = 2.3\ s^{-1}$; the values of $k_{p,\sigma}$ and $k_{t,\sigma}$ are given as a percent of the $k_{p,\mu}$ and $k_{t,\mu}$.

not be obtained and the simulations were performed using a dynamic Monte Carlo model that will not be described here for space limitations.[11]

Figure 8 shows the normal and log-normal distributions for k_p and k_t. This broad distribution of kinetic constants will lead, necessarily, to a polymer with broad CLD and polydispersity index higher than two. It will also make chains to grow and terminate at a different rate on each active site, eliminating the sharp CLD peaks that appear when site activation in fast and all sites have the same polymerization and termination rate constants.

The effect of distributed values for k_p and k_t is clearly illustrated in Figure 9: by increasing the values of the standard deviations for k_p and k_t (given as a percent of their mean values), the CLDs become broader and the sharp peaks disappear completely. This model can, speculatively, explain the time evolution of CLD in stopped-flow reactors and the resulting broad CLD for polymers made with multiple-site catalysts such as heterogeneous Ziegler-Natta catalysts.

Evidently, many more factors may play a role in the dynamic CLD evolution in stopped-flow reactors, notably the influence of mass and heat transfer resistances, as well as mixing non-idealities. This will be the subject of a future publication.

Conclusions

In this article, we proposed two analytical solutions for the dynamic evolution of the chain length distribution of polymers made on stopped-flow reactors (Models 1 and 2) or, more generically, under any conditions where the polymerization time is comparable to the lifetime of the polymer chains. It seems clear that, for a conventional single-site catalysts (or multiple-site catalysts modeled as a superposition of single-site catalysts), instantaneous activation of catalytic sites will lead to chain length distributions that are not observed experimentally. The non-instantaneous activation could be related to a slow (relatively to the residence time in the reactor) site activation rate, as proposed in Model 2, but could also be caused by mass transfer and mixing limitations. Alternatively, a continuous distribution of propagation and chain transfer constants can also further broaden the CLD, as shown through Monte Carlo simulation.

[1] P. J. Flory, *J. Am. Chem. Soc.* **1936**, *58*, 1877.
[2] J. B. P. Soares, L. C. Simon, Coordination polymerization., In: *Handbook of Polymer Reaction Engineering*, T. Meyer, J. Keurentjes, Eds., Wiley-VCH, Weinheim 2005, pp 365–430.
[3] J. B. P. Soares, A. E. Hamielec, *Macromol. React. Eng.* **2007**, *1*, 53.
[4] T. Keii, M. Terano, K. Kimura, K. Ishii, *Makromol. Chem. Rapid Commun.* **1987**, *8*, 583.
[5] B. Liu, H. Matsuoka, M. Terano, *Macromol. Rapid Commun.* **2001**, *22*, 1.
[6] H. Mori, M. Terano, *Trends in Polymer Science* **1977**, *5*, 314.
[7] H. Mori, M. Terano, In: *New Trends in Polyolefin Science and Technology*, S. Hosada, Ed., Research Signpost, Tokyo, Japan **1996**, 37.
[8] A. di Martino, J. P. Broyer, R. Spitz, G. Weickert, T. F. McKenna, *Macromol. Rapid Commun.* **2005**, *26*, 215.
[9] J. B. P. Soares, T. Nguyen, A. E. Hamielec, *Macromol. React. Eng.* **2007**, submitted.
[10] J. B. P. Soares, *Polym. React. Eng.* **1998**, *6*, 225.
[11] T. Nguyen, J. B. P. Soares, *Macromol. React. Eng.* **2007**, submitted.

